TEMPORAL EVOLUTION OF EXTENSIONAL FAULT-PROPAGATION FOLDS

Christopher Jackson[1*], Stephen Corfield[2], Tom Dreyer[3]

[1]*Basins Research Group (BRG), Department of Earth Science and Engineering, Imperial College, Prince Consort Road, London, SW7 2BP, England, UK*

[2]*Corfield Geoscience, 15 Peel Street, Stafford, ST16 2DZ, Stafford, England, UK*

[3]*Statoil ASA, Sandslieveien 90, Bergen 5020, Norway*

[*]*Corresponding author: c.jackson@imperial.ac.uk*

ABSTRACT

Integration of three-dimensional seismic and well data from the Upper Jurassic North Sea rift provides insights into the temporal evolution of fault-propagation folds in extensional settings. The hangingwall of the Oseberg fault zone is characterised by an asymmetric, fault-parallel syncline interpreted as the hangingwall portion of a breached monocline which formed in response to the upward propagation of a normal fault. During the early stage of fault-tip propagation, a growth monocline developed at the depositional surface, resulting in early syn-rift units which thinned and onlapped towards the fault zone. Stratigraphic data from these early syn-rift units suggest that this initial phase of growth folding lasted *ca*. 19 Myr. Late syn-rift units formed an overall faultward expanding wedge, suggesting they were deposited after monocline breaching when a more typical half-graben basin had been established. The results of this study have important implications for assessing the timescale over which fault-propagation folds evolve prior to breaching and the impact of fault-propagation folding on the sequence stratigraphy of syn-rift successions.

Keywords: rift-basin, fault-propagation folding, normal faults, syn-rift

INTRODUCTION

Physical analogue (e.g. Withjack et al. 1990; Withjack & Callaway, 2000) and numerical (e.g. Allmendinger, 1998; Hardy & McClay, 1999; Finch et al. 2004) modelling, in combination with outcrop (e.g. Gawthorpe et al. 1997; Sharp et al. 2000; Jackson et al. 2006) and subsurface studies (e.g. Corfield & Sharp, 2000; Maurin & Niviere, 2000), have demonstrated that fault-propagation folding is an important process during the early stages of fault growth in rift basins. Not only does fault-propagation folding control the geometry of the basin margin through time, but it can also strongly influence the architecture and sequence stratigraphy of coeval syn-rift successions (e.g. Gawthorpe et al. 1997). Despite their obvious importance to the structural and stratigraphic development of rift basins, the evolution of fault-propagation folds and their subsequent impact on the sequence stratigraphy of syn-rift successions remains poorly understood. Whilst physical analogue and numerical models are used to predict the geometric and kinematic evolution of extensional fault-propagation folds, they are unable to explicitly model the timescales over which such structures develop in nature (e.g. Withjack et al. 1990; Hardy & McClay, 1999; Finch et al. 2004). Furthermore, lack of age-constrained growth strata preserved adjacent to fault-propagation folds at outcrop often make it impossible to accurately document the temporal evolution of the structures or to determine their impact on the geometry and sequence stratigraphic variability of coeval syn-rift units (e.g. Khahil & McClay, 2002; Keller & Lynch 2000).

Integration of three-dimensional seismic data and well data provides a valuable method for documenting the temporal evolution of fault-propagation folds and their influence on syn-rift stratigraphy (e.g. see approach utilised by Corfield & Sharp, 2000 and Maurin & Niviere, 2000). Modern three-dimensional seismic data enable the geometry and scale of rift-related faults, folds and associated syn-rift stratigraphy to be accurately determined, whilst well data, integrated with biostratigraphic dating of recognised key stratal surfaces, allow analysis of the syn-rift sequence stratigraphic variability and the timing of the structural development. We present a subsurface analysis of a rift-related normal fault and associated fault-propagation fold from the Upper Jurassic of the North Sea rift basin. The results of this study have important implications for the temporal evolution of fault-propagation folds in rift basins and the sequence stratigraphic variability of the associated syn-rift succession.

REGIONAL STRUCTURAL SETTING AND STRATIGRAPHIC FRAMEWORK

The study area is located on the Horda Platform along the eastern margin of the North Sea rift basin approximately 200 km offshore Norway (Fig. 1). This basin formed in response to Late Jurassic crustal extension which formed a series of fault-blocks bounded by predominantly N-S trending normal faults. The Oseberg fault, which forms the focus of this study, became active in the Early Bathonian and may have involved reactivation of an earlier, basement-involved normal fault related to the preceding Permo-Triassic rift event (Færseth & Ravnås, 1998). Regional studies of this part of the North Sea rift basin have found no evidence for compression during the Late Jurassic post-rift period (Fraser et al. 2003).

The Brent Group was deposited in a marginal to shallow marine environment (e.g. Mitchener et al. 1992) and is typically interpreted to represent a pre-rift unit deposited immediately prior to the Late Jurassic rift event. However, several studies have suggested however that the upper part of the unit may have been deposited during the earliest stage of rifting (Ravnås & Steel, 1997; Davies et al. 2000). The Brent Group (SU1; Figs. 2 and 4) is conformably overlain across a flooding surface dated at 171 Ma by a transgressive syn-rift interval which can be divided into two units. The lower, early syn-rift unit (SU2; Figs. 2, 3A and 4) comprises shallow marine sandstones and shelfal siltstones and mudstones which are separated by a flooding surface. Within the shelfal succession an erosional unconformity dated to span 158-161 Ma is developed. The overlying, late syn-rift unit (SU3; Figs. 2, 3B and 4), which comprises a deep marine succession, overlies the early syn-rift unit across a composite unconformity/flooding surface which spans 152-154 Ma. The top of the syn-rift interval is defined by a regional flooding surface which marks the end of the rift event. Additional wireline and biostratigraphic analysis permits recognition of additional key stratal surfaces and allows both the early and late syn-rift units to be internally subdivided (Fig. 4).

GENERAL STRUCTURAL STYLE OF THE OSEBERG FAULT

The Oseberg fault is planar, strikes N-S, dips steeply (>60°) to the west, and has a maximum displacement of 175 m (Fig. 2). The hangingwall of the Oseberg fault is characterised by an asymmetric, fault-parallel syncline, the axis of which is located 1.6 km westwards of the fault zone. The hangingwall syncline is up to 4.2 km wide and consists of a steeply-dipping (maximum 14°) eastern limb, located in the immediate hangingwall of the Oseberg fault, and a more gently-dipping (2°) opposing limb. A series of moderate displacement (50-70 m) normal faults splay out from the Oseberg fault into its hangingwall. The footwall of the Oseberg fault is poorly-imaged, but units dip either gently westwards towards or gently eastward away from the fault zone. Although this fault-related fold shares many similar geometrical characteristics to fault-propagation folds described from other extensional settings (e.g. Withjack et al. 1990; Gawthorpe et al. 1997; Pascoe et al. 1999; Maurin & Niviere, 2000), the stratal architecture of the associated syn-rift units must be considered before an interpretation of its origin can be proposed.

SYN-RIFT STRATAL ARCHITECTURE

Seismic and well data are integrated to analyse the stratal architecture of the syn-rift basinfill as a tool to determine the origin of the fault-related fold described above. In both data types, focus is placed on syn-rift thickness variations and onlap relationships, observed both within and between stratal units, and in both map-view and cross-section. Three stratal units can be mapped on three-dimensional seismic data in the hangingwall of the Oseberg fault (SU1-3; Figs. 2 and 4). Based on correlation to well data, it is demonstrated that SU1 corresponds to the upper pre-rift unit (169-171 Ma), SU2 to the lower syn-rift unit (151-169 Ma) and SU3 to the upper syn-rift unit (144-151 Ma) (Fig. 4). Although the seismic data allow documentation of the large-scale stratal architecture, the vertical resolution is insufficient to resolve the distribution of the six small-scale stratal units developed within the syn-rift succession. The distribution of these units is analysed using data from the three wells which penetrate the hangingwall syn-rift interval (Fig. 4).

Stratal Unit 1 (SU1 – 169-171 Ma)

Stratal Unit 1 (SU1) is deformed by the fault-parallel fold described above but displays no systematic dip or strike-orientated changes in thickness with respect to the Oseberg fault or associated fold (Fig. 2). This observation is confirmed by well data which indicates that the unit is broadly tabular across the majority of the half-graben, being 52 m in the axis of the hangingwall syncline and thinning to 39 m in the immediate hangingwall of the Oseberg fault due to erosional truncation by overlying units (SU1; Fig. 4). Well data indicates that a flooding surface identified within SU1 is conformable to the top and base of the unit and can be mapped across the entire width of the Omega terrace.

Stratal Unit 2 (SU2 – 151-169 Ma)

In contrast to SU1, SU2 displays marked variations in thickness with respect to the Oseberg fault and its associated fold. Seismic mapping indicates that SU2 thickens eastwards down the hangingwall dipslope and is thickest in the axis of the Omega terrace, but thins eastwards into the immediate hangingwall of the Oseberg fault (Fig. 3A). Thinning of SU2 towards the Oseberg fault is accommodated by onlap of the lowermost seismic reflections onto the steep-dipping, west-facing limb of the hangingwall syncline defined by the top of SU1 (Fig. 2A).

Well data support the seismic observation that SU2 is thickest in the axis of the hangingwall syncline, 1.6 km westwards of the Oseberg fault, and that it thins towards, and is absent in, the immediate hangingwall of the Oseberg fault (Fig. 4). Additionally, well data suggest that eastwards thinning of SU2 is achieved by a combination of onlap onto underlying units (which dip at a shallower angle; Fig. 4) and low-angle truncation beneath overlying units, with key stratal surfaces within SU2 merging towards the fault onto the steep-dipping limb of the hangingwall syncline (Fig. 4). As a result, in the immediate hangingwall of the fault a composite key stratal surface is developed such that the upper syn-rift unit (SU3) directly overlies the uppermost pre-rift unit (SU1) and the early syn-rift unit (SU2) is absent (Fig. 4).

Stratal Unit 3 (SU3 – 144-151 Ma)

Seismic data indicate that along the Oseberg fault zone, SU3 varies between a clear wedge-shaped geometry that thickens eastwards into the immediate hangingwall of the fault and a more tabular geometry that is broadly equal in thickness across the fault block (Fig. 3B). Where a wedge-shaped geometry is observed, westwards thinning of SU3 up the hangingwall dipslope appears to be accommodated by onlap onto the seismic reflection bounding the top of the underlying SU2 (Fig. 2).

The correlation panel, shown in Fig. 4, indicates that SU3 is broadly tabular and at it’s thickest approximately 3.8 km to the west of the Oseberg fault (Fig. 4). SU3 onlaps and oversteps SU2 eastwards towards the Oseberg fault and, in contrast to the underlying unit, is developed in the immediate hangingwall of the fault, where it directly overlies SU1 (Fig. 4). In contrast to those developed in the underlying SU2, key stratal surfaces within SU3, are approximately concordant with the top and base of the unit and show no evidence for convergence eastwards towards the Oseberg fault. Overall, dips within SU3 are quite gentle (<1°; Fig. 4) across the width of the Omega terrace and are typically less than observed in the underlying units (generally >1.5°; Fig. 4).

ORIGIN AND EVOLUTION OF THE OSEBERG FAULT AND FAULT-RELATED FOLD

We consider that four potential models can be proposed for the development of the Oseberg fault and the related fault-parallel fold. Firstly, the fold may have originated in response to post-rift compression of the hangingwall (cf. Knott, 2001), This model is rejected because the observed spatial variability of the syn-rift succession clearly indicates that structural growth was coeval with syn-rift deposition. Furthermore, regional data show no evidence of post-rift compression in this part of the North Sea rift. Secondly, differential compaction of the pre-rift hangingwall succession could have led to the development of a fault-parallel fold adjacent to the Oseberg fault prior to deposition of the syn-rift succession. This is also not considered to be a viable mechanism for fold development as it requires growth of the fold to have been almost instantaneous between the pre and syn-rift units (i.e. post-SU1 and pre-SU2), in the absence of significant loading by the syn-rift succession. Thirdly, frictional drag adjacent to the fault is also rejected as a viable mechanism for the formation of the fault-related fold, as such drag folds are typically an order of magnitude narrower (i.e. 10-100's of metres) than the fold described here.

Based on the scale of the fold and the architecture of the associated syn-rift succession, our final and preferred model for the origin of the fault-related fold in the hangingwall of the Oseberg fault is as a fault-propagation fold which initially developed above an upwardly-propagating fault. Based on the architecture and dating of the syn-rift succession, temporal constraints can be placed on the onset, duration and cessation of fault-propagation folding. During deposition of SU1, the Oseberg fault is interpreted to have been inactive as suggested by the tabular geometry of this unit across the width of the hangingwall (Fig. 5). It should be noted that the fault may have been active at depth but did not influence at-surface topography or the resultant syn-rift architecture. At-surface growth folding began at 169 Ma at the start of deposition of SU2 as indicated by thinning and onlap of this unit towards the fault onto the steep, westwards-dipping limb of the hangingwall syncline. The site of maximum subsidence and hence sediment accumulation was located in the synclinal, fault-parallel depocentre offset 2.8 km from future position of the Oseberg fault (SU2; Figs. 2, 3B and 5). Incremental fault slip, fold amplification and rotation of previously deposited syn-rift units resulted in the formation of progressive unconformities (see discussion below) whereby successive key stratal surfaces (flooding surface and erosional surfaces) surfaces merge towards the growing structure. Similar geometries have been documented adjacent to growing structures in both extensional (e.g. Maurin & Niviere, 2000) and compressional structures (e.g. Ford et al. 1997; Gawthorpe et al. 2000).

In contrast to SU2, the late syn-rift unit (SU3) thickens towards the Oseberg fault, suggesting that the fault had breached the fault-propagation fold and from 151 Ma onwards was a surface-breaking feature (Fig. 5). Breaching of the fault-propagation fold, possibly augmented by uplift in the footwall to the fault bounding the western margin of the fault block, resulted in eastwards rotation of the hangingwall dipslope as indicated by westwards onlap of SU2 onto the hangingwall dipslope (Fig. 5). This change in structural style was associated with a migration in the locus of maximum subsidence and sediment accumulation eastwards towards the immediate hangingwall of the Oseberg fault (Fig. 5). Thinning of the late syn-rift unit along portions of the Oseberg fault (e.g. Fig. 4) suggests that although the fault-propagation fold had been breached, the steep-dipping limb of the hangingwall syncline locally still had a topographic expression in the hangingwall of the fault. The Oseberg fault persisted as a surface-breaking feature until the end of rifting at 144 Ma.

DISCUSSION

Our study places broad temporal constraints on the potential duration of fault-propagation folding during normal fault growth, and suggests that in the present study area at-surface growth folding characterised the initial *ca*. 19 My of activity on the Oseberg fault before the fold was fully breached along its length. The Revfallet fault, offshore Mid-Norway (Pascoe et al. 1999; Corfield & Sharp, 2000) and the western margin of the Rhine Graben (Maurin & Niviere, 2000) are two areas where the temporal evolution of fault-propagation folding has also been resolved using the coeval syn-rift architecture. Fault-propagation folding along the Revfallet fault was ongoing for *ca*. 24 Myr and the fold was only locally breached, whereas in the Rhine Graben the duration of the fault-propagation folding prior to fold breaching can be dated to have lasted *ca*. 3.5 Myr. The marked variability in the duration of fault-propagation folding demonstrated by these examples and the present study may reflect the rate at which the basin-bounding fault propagates, the strength of the cover stratigraphy or the degree of coupling of faulting at depth and folding in the cover as suggested by physical analogue (e.g. Withjack et al. 1990; Withjack & Callaway, 2000) and numerical models (e.g. Hardy & McClay, 1999; Finch et al. 2004). For example, along the Revfallet fault a thick evaporite horizon at the base of the sedimentary cover sequence inhibited the upward propagation of the basin-bounding fault, hence (i) the relative longevity of fault-propagation folding (e.g. *ca*. 24 Myr) and (ii) only local breaching of the fault-propagation fold along-strike (cf. Withjack & Callaway, 2000). In contrast, the relatively short duration of fault-propagation folding indicated by the Rhine Graben example may reflect the rapid upward propagation of the fault through a brittle carbonate-dominated cover sequence which contains only thin evaporite horizons.

Fault-propagation folding also markedly affected the stratigraphic development of the syn-rift basinfill. In addition to controlling the large-scale architecture of the syn-rift succession, fault-propagation folding also strongly influenced the spatial development of key stratal surfaces within the syn-rift. For example, syn-rift unconformities become increasing erosional towards the crest of the fault-propagation fold and accordingly represent increasingly larger periods of time and missing strata. Conversely, the unconformities become suppressed in the hangingwall syncline where subsistence and hence accommodation was greater (e.g. within SU2; Fig. 4). One consequence of unconformities becoming enhanced towards the evolving fault-propagation fold is that marine flooding surfaces during the early syn-rift are restricted to the hangingwall syncline axis due to later erosion beneath syn-rift unconformities. Only during the late syn-rift when subsidence and accommodation in greater in the immediate hangingwall do marine flooding surfaces become more areally widespread. Clearly such temporal and spatial variability of key stratal surface development has major implications for correlating such surfaces over relatively short (i.e. 1-3 km) length-scales (cf. Gawthorpe et al. 1997; 2000).

ACKNOWLEDGMENTS

Rob Gawthorpe, Mike Young and Mark Scott are thanked for discussions during this study. Norsk Hydro are thanked for permission to publish the results of this study.

REFERENCES

Allmendinger, R.W., 1998, Inverse and forward numerical modelling of tri-shear fault-propagation folds: Tectonics, v. 17, p. 62-81.

Corfield, S.C., and Sharp, I.R., 2000, Structural style and stratigraphic architecture of fault propagation folding in extensional settings: a seismic example from the Smørbukk area, Halten Terrace, Mid-Norway: Basin Research, v. 12, p. 329-341.

Davies, S.J., Dawers, N.H., McLeod, A.E., and Underhill, J.R., 2000, The structural and sedimentological evolution of early syn-rift successions: the Middle Jurassic Tarbert Formation, North Sea: Basin Research, v. 12, p. 343-365.

Finch, E., Hardy, S., and Gawthorpe, R.L., 2004, Discrete-element modelling of extensional fault-propagation folding above rigid basement fault blocks: Basin Research, v. 16, p. 467-488.

Ford, M., Williams, E.A., Artoni, A., Verges, J., and Hardy, S., 1997, Progressive evolution of a fault-related fold pair from growth strata geometries, Sant Llorenc de Morunys, SE Pyrenees: Journal of Structural Geology, v. 19, p. 413-441.

Færseth, R. B., and Ravnås, R., 1998, Evolution of the Oseberg fault block in context of the northern North Sea structural framework: Marine and Petroleum Geology, v. 15, p. 467-490.

Gawthorpe, R.L., Sharp, I.R., Underhill, J.R., and Gupta, S., 1997, Linked sequence stratigraphic and structural evolution of propagating normal faults: Geology, v. 25, p. 795-798.

Gawthorpe, R.L., Hall, M., Sharp, I.R., and Dreyer, T., 2000, Tectonically enhanced forced regressions: examples from growth folds in extensional and compressional settings, the Miocene of the Suez Rift and the Eocene of the Pyrenees, *in* Hunt, D., and Gawthorpe, R.L., eds., Sedimentary responses to forced regressions: Geological Society (London) Special Publication 172, p. 177-192.

Hardy, S., and McClay, K., 1999, Kinematic modelling of extensional fault-propagation folding: Journal of Structural Geology, v. 21, p. 695-702.

Jackson, C.A.L., Gawthorpe, R.L., and Sharp, I.R., 2006, Style and sequence of deformation during extensional fault-propagation folding: examples from the Hammam Faraun and El-Qaa fault blocks, Suez Rift, Egypt: Journal of Structural geology, v. 28, p. 519-535.

Keller, J.V.A., and Lynch, G., 2000, Displacement transfer and forced folding in the Maritimes basin of Nova Scotia, eastern Canada, *in* Cosgrove, J.W., and Ameen, M.S., eds., Forced folds and fractures: Geological Society (London) Special Publication 169, p. 87-101.

Khalil, S.M., and McClay, K.R., 2002, Extensional fault-related folding, northwestern Red Sea, Egypt: Journal of Structural Geology, v. 24, p. 743-762.

Knott, S.D., 2001, Gravity-driven crustal shortening in failed rifts: Journal of the Geological Society of London, v. 158, p. 193-196.

Maurin, J-C., and Niviere, B., 2000, Extensional forced folding and décollement of the pre-rift series along the Rhine Graben and their influence on the geometry of the syn-rift sequences, *in* Cosgrove, J.W., and Ameen, M.S., eds., Forced folds and fractures: Geological Society (London) Special Publication 169, p. 73-86.

Mitchener, B.C., Lawrence, D.A., Partington, M.A., Bowman, M.B.J., and Gluyas, J., 1992, Brent Group: sequence stratigraphy and regional implications, *in* Morton, A.C., Haszeldine, R.S., Giles, M.R., and Brown, S., eds., Geology of the Brent Group: Geological Society (London) Special Publication 61, p. 45-80.

Pascoe, R., Hooper, R., Storhaug, K., and Harper, H., 1999, Evolution of extensional styles at the southern termination of the Nordland Ridge, mid-Norway: a response to variations in coupling above Triassic salt, *in* Fleet, A.J., and Boldy, S.A.R., eds., Petroleum Geology of Northwest Europe Proceedings of the 5th Conference, pp. 83-90.

Ravnås, R., and Steel, R.J., 1997, Contrasting styles of Late Jurassic syn-rift turbidite sedimentation: a comparative study of the Magnus and Oseberg areas, northern North Sea: Marine and Petroleum Geology, v. 14, p. 417-449.

Sharp, I.R., Gawthorpe, R.L., Underhill, J.R., and Gupta, S., 2000, Fault propagation folding in extensional settings: examples of structural style and syn-rift sedimentary response from the Suez Rift, Egypt: Geological Society of America Bulletin, v. 112, p. 1877-1899.

Withjack, M.O., Olson, J., and Peterson, E., 1990, Physical models of extensional forced folds: American Association of Petroleum Geologists Bulletin, v. 74, p. 1038-1054.

Withjack, M.O., and Callaway, S., 2000, Active normal faulting beneath a salt-layer: physical study of deformation patterns in the cover sequence: American Association of Petroleum Geologists, v. 84, p. 627-651.

FIGURE CAPTIONS

Figure 1. Map indicating the location of the study area in the North Sea. The locations of wells used in this study and Fig. 3 are also shown.

Figure 2. Representative (time-migrated) seismic section across the Omega Terrace flattened on the top of SU3 (top syn-rift) indicating the geometry of the fault-propagation fold and associated stratal units. Location of seismic section is shown in

Fig. 3. Seismic horizons which were mapped and used to construct Figs. 3A and 3B are marked. Black represents a downward increase in acoustic impedance and data is zero-phase.

Figure 3. A: Seismic isochron map of SU2. B: Seismic isochron map of SU3. Scale is in millisecond (ms) two-way traveltime (TWTT). Locations of Figs. 2 and 4 are shown.

Figure 4. Well-based correlation across the eastern part of the Omega terrace illustrating the architecture of stratal units associated with the fault-propagation fold. Locations of wells used are shown in Fig. 3. GR = gamma-ray and scale is from 0 (left) to 150 (right) API. Ages of selected key stratal surfaces are shown.

Figure 5. Schematic reconstruction indicating the evolution of the fault-propagation fold and variability in stratal architecture and key stratal surface development. A: Early syn-rift – SU2 (151-169 Ma). B: Late syn-rift – SU3 (144-151 Ma). See text for full discussion. Key to stratigraphic units and key stratal surfaces is the same as in Fig. 4. Note that details of key stratal surface development are only shown for the interval considered.

Fig. 1

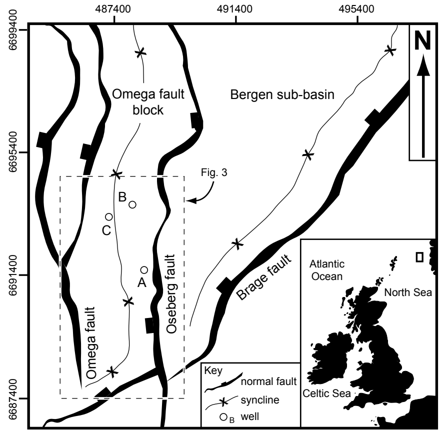

Figure 1. Map indicating the location of the study area in the North Sea. The locations of wells used in this study and Fig. 3 are also shown.

Fig. 2

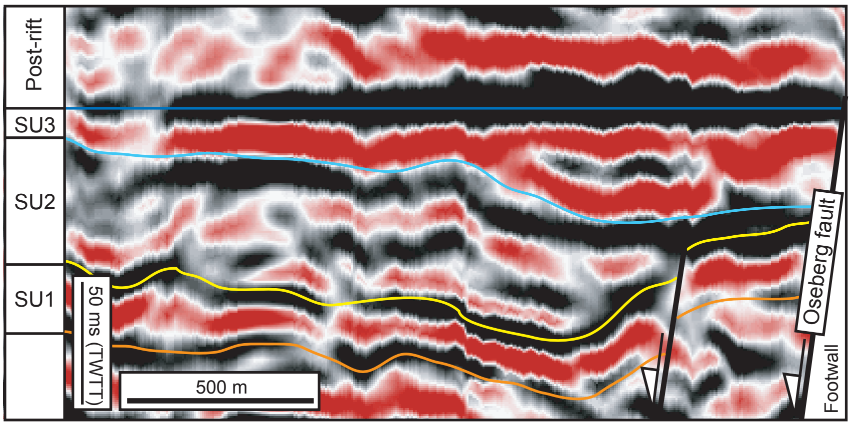

Figure 2. Representative (time-migrated) seismic section across the Omega Terrace flattened on the top of SU3 (top syn-rift) indicating the geometry of the fault-propagation fold and associated stratal units. Location of seismic section is shown in Fig. 3. Seismic horizons which were mapped and used to construct Figs. 3A and 3B are marked. Black represents a downward increase in acoustic impedance and seismic data is zero-phase. Note the minor fault developed in the hangingwall of the Oseberg fault.

Fig. 3

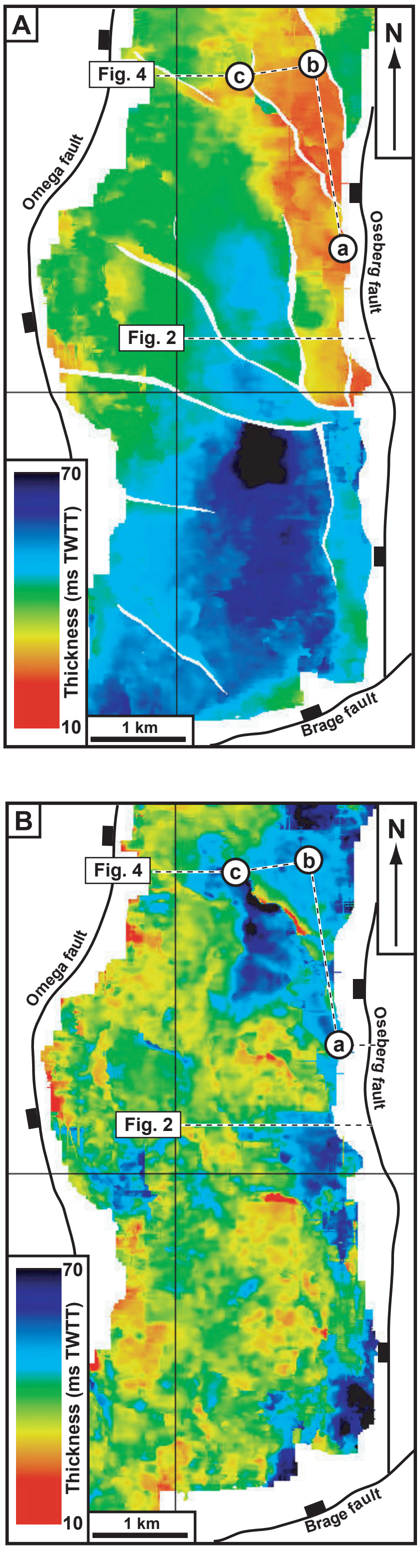

Figure 3. A: Seismic isochron map of SU2. B: Seismic isochron map of SU3. Scale is in millisecond (ms) two-way traveltime (TWTT). Locations of Figs. 2 and 4 are shown.

Fig. 4

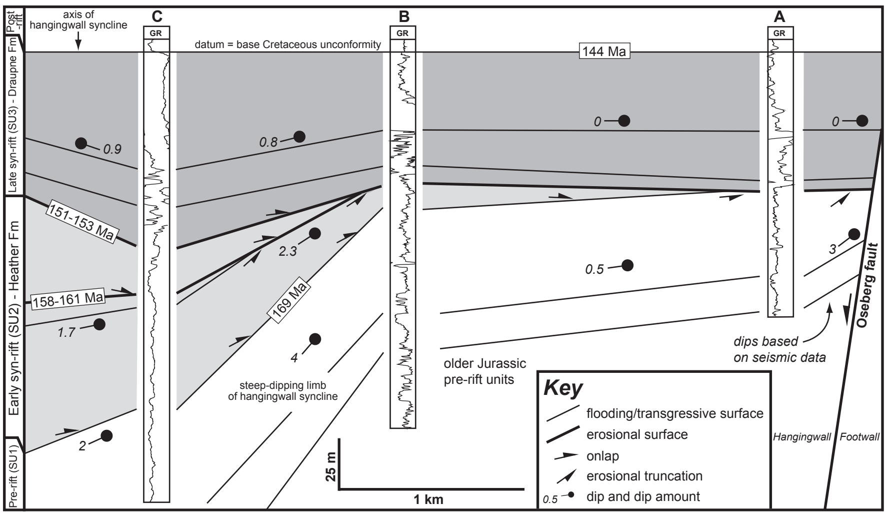

Figure 4. Well-based correlation across the eastern part of the Omega terrace illustrating the architecture of stratal units associated with the fault-propagation fold. Locations of wells used are shown in Fig. 3. GR = gamma-ray and scale is from 0 (left) to 150 (right) API. Ages of selected key stratal surfaces are shown.

Fig. 5

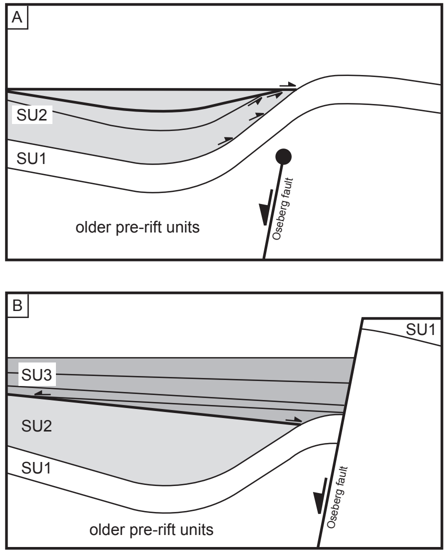

Figure 5. Schematic reconstruction indicating the evolution of the fault-propagation fold and variability in stratal architecture and key stratal surface development. A: Early syn-rift – SU2 (151-169 Ma). B: Late syn-rift – SU3 (144-151 Ma). See text for full discussion. Key to stratigraphic units and key stratal surfaces is the same as in Fig. 4. Note that details of key stratal surface development are only shown for the interval considered and only the main Oseberg fault is shown for clarity.